# Flight Data Recorder for an American Football

Chris J. Nowak
*General Dynamics Advanced Information Engineering Services, Buffalo, NY, USA*
Venkat Krovi, William J. Rae
*Mechanical and Aerospace Engineering, University at Buffalo, The State University of New York, Buffalo, NY USA*

***Abstract***: The increasing availability of small-scale, fast-response instrumentation has contributed both to improved equipment and better training methods in several sports, such as golf. In contrast, the game of football has not seen comparable advances, in part because the flight of a football entails a complex interaction between gyroscopic and aerodynamic loads (Rae 2003). At present, determination of the aerodynamics by wind-tunnel testing is incomplete, and there are essentially no data available from flights observed by calibrated cameras at known locations. In this paper, we discuss our efforts towards the development of a low-cost onboard flight-data recorder to capture the free-flight dynamics for the American Football.

The final system was intended to be capable of onboard logging of the six components of acceleration during free flight and for post-flight downloading and further processing to identify the corresponding forces and torques. Limitations on total physical mass and mass distribution, availability of suitable sensors, feasible sensor locations and electronic interfaces, achievable sampling rates and post-flight data-processing requirements placed stringent constraints on the design of the overall system. The final configuration was successful in meeting these constraints and a proof-of-concept prototype measurement system, suitable for mounting within the football, was developed by interfacing PIC16F876 microcontrollers to accelerometers and electronic storage devices. Recorded data from this experimental prototype show qualitative agreement with six degree of freedom simulations. The results also show clearly the steps needed for a second-generation system, as discussed in the Concluding Remarks.

**Introduction**

The flight of any sports ball takes place in two phases: a launch phase during which the athlete imparts translational and angular accelerations to the ball, followed by a free-flight phase whose accelerations are dictated by aerodynamic and gravitational forces. For impact-driven balls, studies of the launch phase often require only simple collision mechanics (Adair 1990), while soccer balls, rugby balls, and footballs experience a more extensive time history of the launch acceleration (Asai et al 2002, Carre et al 2002, Brancazio 1984). Wind-tunnel data on the aerodynamic loads encountered in flight are quite extensive for spheres (Mehta 1985), but are still far from complete for footballs: even for a quantity as fundamental as the drag coefficient at zero wind angle, the papers of Watts and Moore 2003 and of Rae and Streit 2002 differ by a factor of two or more.

The approach taken in the present paper reflects the authors' conclusion that use of onboard sensors in a thrown ball offers advantages not easily attainable in wind-tunnel testing, where spin causes large model accelerations and where the test envelope must include a very large range of wind angles. Moreover, integration of the measured accelerations offers the hope of acquiring accurate trajectory data and detailed information about the throwing motion itself. This approach has its own problems, of course, among them requirements for the accuracy of the data, provision for data storage and downloading, and data-reduction procedures that account for mass distributions different from those of a non-instrumented ball. The paragraphs below report a first attempt to explore these requirements. These sections include a description of the system used, the data obtained, and the data-reduction scheme envisioned for extracting the aerodynamic loads. The goal of this work was to determine whether useful data could be obtained within the constraints of current electromechanical technology. The conclusion reached is an affirmative one, and the concluding remarks contain some suggestions of areas where further development is needed.

**The System Used**

The sensor chips (Analog Devices ADXL250) carried accelerometers which measured acceleration components in two orthogonal directions in the plane of the chip (Nowak 2003). The signals from four such chips (eight channels in all) were filtered and sent to an analog-to-digital converter contained on one of two PIC 16C876 microprocessors, and the 8-bit digital signals from each chip were stored on a corresponding Serial EEPROM (AT25640). The signals were stored at 5 millisecond intervals. Data acquisition was started by a slide switch, and data were taken for a period of ten seconds, irrespective of the flight duration. Following this, the data were downloaded to an Excel file for further processing. The microprocessor was programmed in PicBasicPro, using Code Designer Lite.

The sensors were mounted on two printed-circuit boards which were slotted in such a way as to allow assembly as an orthogonal pair whose axis of intersection was aligned with the major axis of the ball. The ball itself, shown in Fig. 1, was a Nerf™ ball, from which the rubber foam was partially removed so as to accept the assembled boards, two 9-volt batteries, and associated cables. Each of the two PC boards carried two accelerometer chips, mounted as shown in Fig. 2. These locations are denoted by the symbols A, B, C, and D.

**Results**

Following assembly of the ball, several throws were made in order to examine the quality of the data. Figure 3 shows the outputs from chip D. The upper (dotted-line) trace is the $x_B$ (axial) component of the acceleration and the lower (solid-line) trace is the $y_B$ (radial) component. The first thing to be noted is the transition from the launch phase to the free-flight phase at around 0.4 seconds. The upper trace shows a monotonically increasing axial acceleration while the ball is being held, which changes during free flight to an oscillation at nearly constant amplitude and slowly decreasing frequency. The lower trace shows very little radial acceleration during launch, followed during flight by a large negative acceleration (zero acceleration corresponds to 128 counts) whose magnitude decreases slowly. These free-flight features are what one would expect, namely that the upper trace indicates a " wobble" oscillation, while the lower trace represents a centripetal acceleration arising from the spin angular velocity.

These interpretations can be put on a more quantitative basis as follows. Consider first the lower trace; using the nominal sensitivity (128 acceleration counts equals 50 g's) yields an acceleration around 10 g's at a one-inch radius. Using $a = w^2 r$ ,this indicates an angular velocity around 62 $rdn/s^2$ or about 600 RPM, a typical spin rate for a thrown football. The fact that this rate is decreasing with time may be a symptom of an antispin torque, but it might also be connected to the changing orientation of the ball. The data-reduction considerations described below suggest that more information is needed in order to establish the source of the decay.

The frequency of the upper-trace oscillation is approximately 340 RPM over the 3-second flight. This corresponds quite closely with a spin-to-wobble ratio of 1.8, the value known both experimentally and analytically (Rae 2003) to apply to forward passes. The fact that the wobble frequency decreases slightly toward the end of the flight is consistent with the decaying RPM seen in the centripetal-acceleration signal.

**Data Reduction**

The interpretation of results given in the previous section is described as qualitative, since there are too few channels of data to define uniquely the relations between the signals displayed and the corresponding state-vector variables. To further clarify this point, this section contains a brief presentation of the procedure envisioned for extracting the state variables from a more complete set of accelerometer signals.

Consider the motion of an accelerometer located at point $T$ fixed in a rigid body which is experiencing both linear and angular accelerations. The vector velocity of the point is

$$\vec{V}_T = \vec{V}_{CM} + \vec{w} \times \vec{R} \qquad (1)$$

where $\vec{V}_{CM}$ denotes the velocity of the center of mass, $\vec{w}$ the angular velocity of the rigid body, and $\vec{R}$ the position vector from the center of mass to the point $T$. The translational and angular velocities are time-dependent. This equation will have different components when resolved in different coordinate systems. Let $(\ )_F$ denote resolution into components along space-fixed (inertial) axes and $(\ )_B$ into body-fixed (moving) axes. Both sets of axes have their origin at the center of mass, as shown in Fig. 4, which contains the definitions of the translational-velocity, angular-velocity, force, and torque components in the two axis systems. Velocity components in the two axis systems are related by

$$\vec{V}_{T,F} = \left[m_{ij}\right]\vec{V}_{T,B} \quad \text{or} \quad \begin{Bmatrix} V_{T,XF} \\ V_{T,YF} \\ V_{T,ZF} \end{Bmatrix} = \begin{bmatrix} m_{11} & m_{12} & m_{13} \\ m_{21} & m_{22} & m_{23} \\ m_{31} & m_{32} & m_{33} \end{bmatrix} \begin{Bmatrix} u \\ v \\ w \end{Bmatrix} \qquad (2)$$

where the coordinate-transformation matrix $\left[m_{ij}\right]$ depends on the orientation of the body axes with respect to the space-fixed axes and on the variables chosen to define the orientation (for example, the Euler Angles - see Nelson 1998 and Fig. 5).

Taking the time derivative of Eqn (2) yields the acceleration components of the point $T$, resolved in body coordinates, as:

$$\begin{aligned} a_{XB} &= \dot{u} - rv + qw - x_B(q^2 + r^2) + y_B(pq - \dot{r}) + z_B(pr + \dot{q}) \\ a_{YB} &= \dot{v} + ru - pw + x_B(pq + \dot{r}) - y_B(p^2 + r^2) + z_B(qr - \dot{p}) \\ a_{ZB} &= \dot{w} - qu + pv + x_B(pr - \dot{q}) + y_B(rq + \dot{p}) - z_B(p^2 + q^2) \end{aligned} \qquad (3)$$

Note that the scalar components of the acceleration experienced at a general point $(x_B, y_b, z_B)$ contain contributions from the motion of the center of mass plus Coriolis, centripetal, and angular-acceleration terms proportional to the vector displacement of the point in question from the center of mass.

The interpretation given above of the lower trace in Fig. 3 is based on the assumption that the term $y_B p^2$ is the dominant one, but the presence of the other terms prompts caution in drawing any firm conclusions about the mechanism causing the amplitude decay of that signal, especially since the distances $x_B$ and $z_B$, though small, were nonzero.

The concept for a six degree of freedom system is to mount pairs of accelerometers on three mutually perpendicular planes: an $x_B, y_B$ plane carrying a pair at $x_B, y_B, z_B = (0, \pm b, 0)$, an

$x_B, z_B$ plane carrying a pair at $x_B, y_B, z_B = (\pm a, 0, 0)$ and a $y_B, z_B$ plane carrying a pair at $x_B, y_B, z_B = (0, 0, \pm c)$. Then the signals from the $x_B, y_B$ plane can be combined as

$$\begin{aligned}
\sum a_x(\pm b) &\equiv a_{xB}(0,+b,0) + a_{xB}(0,-b,0) = 2(\dot{u} - rv + qw) \\
\sum a_y(\pm b) &\equiv a_{yB}(0,+b,0) + a_{yB}(0,-b,0) = 2(\dot{v} + ru - pw) \\
\Delta a_x(\pm b) &\equiv a_{xB}(0,+b,0) - a_{xB}(0,-b,0) = 2b(pq - \dot{r}) \\
\Delta a_y(\pm b) &\equiv a_{yB}(0,+b,0) - a_{yB}(0,-b,0) = -2b(p^2 + r^2)
\end{aligned} \qquad (4)$$

Similar combinations of signals from the other two planes give more than enough equations for the integration of $\dot{u}, \dot{v}, \dot{w}, \dot{p}, \dot{q},$ and $\dot{r}$.

**Concluding Remarks**

This investigation shows that it is possible to record data from accelerometers mounted in a thrown football at a frequency well above the Nyquist level corresponding to the spin rate, and that the signals are, qualitatively, what one would expect. These results offer encouragement to proceed to a second-generation build designed to yield quantitative results. This will require use of a regulation-size ball, a larger number of sensors, greater data-storage capacity, and perhaps increased precision of the analog-to-digital conversion.

With these improvements, it will be possible to address a number of issues in the data-reduction process, among them the algorithm used for integration of the equations for $\dot{u}, \dot{v}, \dot{w}, \dot{p}, \dot{q},$ and $\dot{r}$, including the presence of small but nonzero terms arising from the precise locations of the accelerometers. Assuming that the state vector can be found as a function of time, estimation of the aerodynamic loads can then proceed, but it will require accounting for the full inertia tensor and center-of-gravity location of the instrumented ball. All of these factors will present interesting challenges to improved accuracy in understanding the flight of sports balls in general and of footballs in particular.

***References***


Adair, R. K. (1990) *The Physics of Baseball*, Harper and Row, New York

Asai, T., Carre, M. J., Akatsuka, T., and Haake, S. J. (2002) The Curve Kick of a Football I: Impact with the Foot, *Sports Engineering*, **5,** 183 - 192

Brancazio, P. J. (1984) *Sport Science*, Simon and Schuster, New York

Carre, M. J., Asai, T., Akatsuka, T., and Haake, S. J. (2002) The Curve Kick of a Football II: Flight through the Air, *Sports Engineering*, **5**, 193 - 200

Mehta, R. D. (1985) Aerodynamics of Sports Balls. In: *Annual Review of Fluid Mechanics*, **17**,[eds. M. D. VanDyke, J. V. Wehausen, and J. L. Lumley], pp. 151-180. Annual Reviews, Inc, Palo Alto

Nelson, R. C. (1998) *Flight Stability and Automatic Control*, 2nd Ed., McGraw-Hill, Boston

Nowak, C. J. (2003) *Flight Data Recorder for the American Football*. Master of Engineering Project Report, University at Buffalo

Rae, W. J. and Streit, Robert J. (2002) Wind-Tunnel Measurements of the Aerodynamic Loads on an American Football, *Sports Engineering*, **5**, 165 - 172

Rae,W. J.(2003) Flight Dynamics of an American Football in a Forward Pass, *Sports Engineering* , **6**, 149 - 164

Watts, R. G., and Moore, G. (2003) The Drag Force on an American Football, *American Journal of Physics*, **71**, 791-793

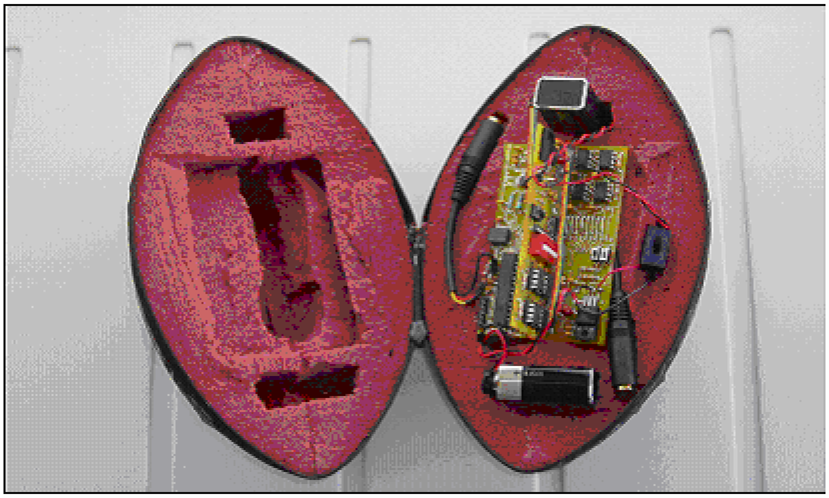

*Fig.* 1 Flight Data Recorder

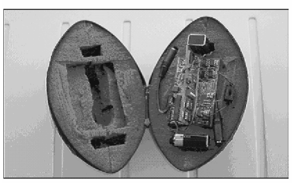

*Fig.* 1 Flight Data Recorder

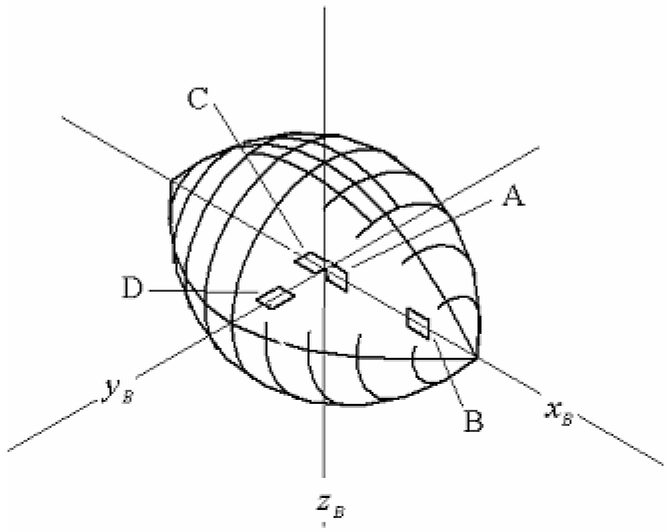


*Fig. 2* Accelerometer Locations

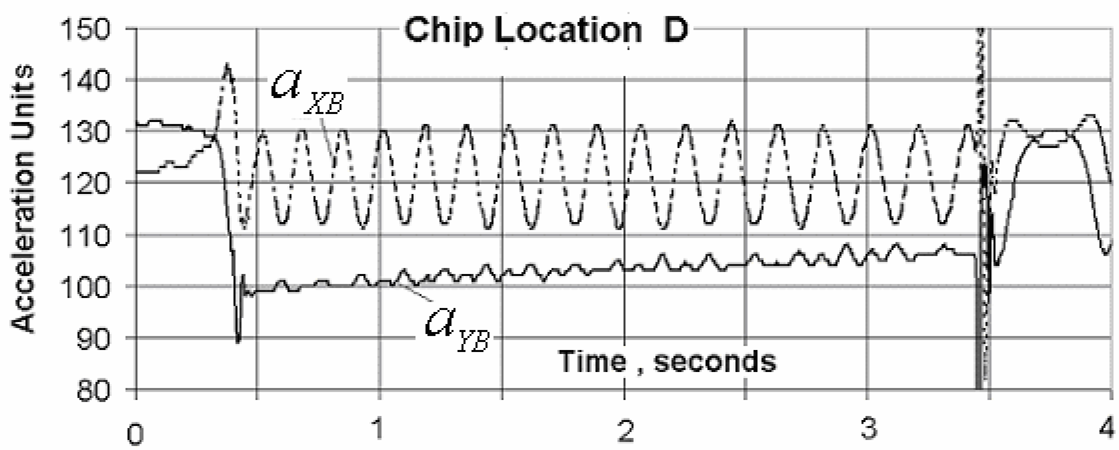


*Fig. 3* Accelerometer Data for a Forward Pass

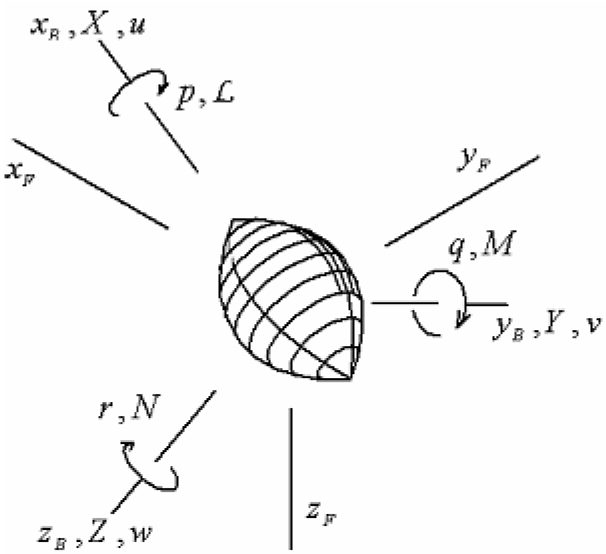


*Fig. 4* Definitions of Vector Quantities

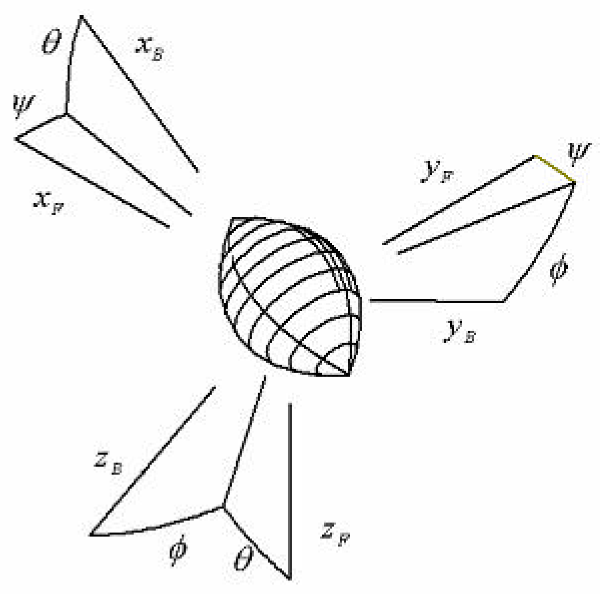


*Fig. 5* Euler Angles